Published in final edited form as:
Neuron. 2013 January 9; 77(1): 43–57. doi:10.1016/j.neuron.2012.10.037.

Nuclear calcium signaling in spinal neurons drives a genomic program required for persistent inflammatory pain

Manuela Simonetti[1,Ψ], **Anna M. Hagenston**[2,Ψ], **Daniel Vardeh**[1,Ψ], **H. Eckehard Freitag**[2,Ψ], **Daniela Mauceri**[2,Ψ], **Jianning Lu**[1], **Venkata P. Satagopam**[3], **Reinhard Schneider**[3,4], **Michael Costigan**[5], **Hilmar Bading**[2,*], and **Rohini Kuner**[1,*]

[1]Institute for Pharmacology, University of Heidelberg, Im Neuenheimer Feld, Heidelberg, 69120 Germany

[2]Department of Neurobiology, Interdisciplinary Center for Neurosciences, University of Heidelberg, Heidelberg, 69120 Germany

[3]Structural and Computational Biology Unit, European Molecular Biology Laboratory (EMBL), Meyerhofstrasse 1, D-69117 Heidelberg, Germany

[4]LUXEMBOURG CENTRE FOR SYSTEMS BIOMEDICINE (LCSB), University of Luxembourg, Campus Belval, House of Biomedicine, 7-avenue des Hauts-Fourneaux, L-4362 Esch sur Alzette, Luxembourg

[5]F.M. Kirby Neurobiology Center, Children's Hospital Boston and Harvard Medical School, Boston, MA 02115, USA

Summary

Persistent pain induced by noxious stimuli is characterized by the transition from normosensitivity to hypersensitivity. Underlying mechanisms are not well understood, although gene expression is considered important. Here we show that persistent nociceptive-like activity triggers calcium transients in neuronal nuclei within the superficial spinal dorsal horn, and that nuclear calcium is necessary for the development of long-term inflammatory hypersensitivity. Using a nucleus-specific calcium signal perturbation strategy *in vivo* complemented by gene profiling, bioinformatics and functional analyses, we discovered a pain-associated, nuclear calcium-regulated gene program in spinal excitatory neurons. This includes C1q, a novel modulator of synaptic spine morphogenesis, which we found to contribute to activity-dependent spine remodelling on spinal neurons in a manner functionally associated with inflammatory hypersensitivity. Thus, nuclear calcium integrates synapse-to-nucleus communication following noxious stimulation and controls a spinal genomic response that mediates the transition between acute and long-term nociceptive sensitization by modulating functional and structural plasticity.

*Correspondence should be addressed to H.B. at Hilmar.Bading@uni-hd.de or to R. K. at rohini.kuner@pharma.uni-heidelberg.de.
ΨThese authors contributed equally to the study.

ACCESSION NUMBERS

Complete profiling data have been uploaded in the public domain with the accession number E-MTAB-1416.

Introduction

Peripheral and central neural networks mediating the complex experience of pain show various forms of plasticity in pathological disease states over diverse temporal and anatomical scales, leading to exaggerated responses to noxious stimuli (hyperalgesia) and may contribute to aberrant pain sensation in response to non-noxious sensory inputs (allodynia) (Kuner, 2010; Sandkühler, 2009). Despite recent advances, the molecular basis of transition between acute sensitization and long-term hypersensitivity is not well understood. Tremendous potential for long-term plasticity lies in the ability of synaptic nociceptive mediators and cellular modulators to trigger changes in gene expression (Woolf and Costigan, 1999). Addressing how local synaptic events are spatio-temporally linked to the modulation of gene expression in pain networks is therefore important for understanding sensitization mechanisms.

Recent studies have revealed important insights into routes for synapse-to-nucleus communication in the context of neuronal survival and long-term memory (Hagenston and Bading, 2011). Calcium signals couple synaptic activity to the regulation of gene transcription and thus serve as mediators of the dialogue between synapses and the nucleus (Hardingham et al., 2001; Bengtson et al., 2010). Nuclear calcium acting primarily via nuclear calcium/calmodulin-dependent (CaM) protein kinases II and IV regulates genomic programs, that have been studied in the context of neuronal survival, synaptic plasticity and memory formation, particularly in hippocampal neurons (Limbäck-Stokin et al., 2004; Zhang et al., 2007, 2009; Mauceri et al., 2011; Oliveira et al., 2012). The cyclic AMP response element binding protein (CREB), a major target of nuclear calcium-CaMKIV signaling (Hardingham et al., 1997; Hardingham et al., 2001), can bind to and influence the activity of 4000 to 6000 promoter sites in the rat or human genomes (Impey et al., 2004). Nuclear calcium-CaMKIV signaling also regulates the activity of the transcriptional co-activator CREB binding protein (CBP) (Hagenston and Bading, 2011) that interacts with CREB but also with a number of other DNA binding proteins (Vo and Goodman, 2001). Furthermore, nuclear calcium also initiates genome wide modifications of the chromatin state in response to synaptic activity, e.g. via CaMKII-mediated phosphorylation of Methyl-CpG-binding Protein 2 (MeCP2) on its activator site serine 421 (Buchthal et al., 2012) or transcriptional induction of the *de novo* DNA methyltransferase, Dnmt3a2 (Oliveira et al., 2012).

Previous studies have reported roles for many transcriptional regulators including CREB and MeCP2 in nociceptive plasticity (Fang et al., 2002; Ji et al., 1999; Geranton et al., 2007). However, little is known about the potential for nociceptive activity to trigger nuclear calcium signaling and it remains unknown whether nuclear calcium serves as a signaling end point in pain-associated synapse-to-nucleus communication.

Here we show that persistent nociceptive-like activity triggers calcium transients in the nuclei of spinal dorsal horn neurons, which play a key role in the development of persistent inflammatory pain, but not in the basal pain sensitivity or the acute sensitization evoked by nociceptive inputs. A genome-wide transcriptome analysis uncovered a distinct spinal gene pool directly regulated by nuclear calcium that not only includes a large set of known, key pain-related genes, but also novel plasticity-related genes and regulators of spinal dendritic spine remodeling. Thus, functional and structural plasticity governed by a nuclear calcium-driven genomic response is a key intermediate step linking nociceptive activity and the development of long-lasting hypersensitivity.

Results

Viral-mediated delivery of tools for analyzing nuclear calcium signaling in the mouse spinal cord *in vivo*

We used recombinant adeno-associated virus (rAAV)-mediated gene delivery (During et al., 2003) to overexpress molecular tools for either imaging or quenching nuclear calcium signals. Our objective was to specifically target excitatory neurons in the superficial spinal laminae that receive and process nociceptive information from peripheral sensory afferents and then subsequently project this information to the brain. Nuclear calcium signaling was blocked by means of expression of Calmodulin binding protein 4 (CaMBP4), a nuclear protein that contains 4 repeats of the M13 calmodulin-binding peptide derived from the rabbit skeletal muscle myosin light chain kinase, which has been characterized previously (Wang et al., 1995 Zhang et al., 2007; Zhang et al., 2009, Mauceri et al. 2011). CaMBP4 does not buffer calcium, but instead binds calcium-bound calmodulin and prevents the activation of downstream signaling cascades. It's effects on synaptic activity-dependent transcription that is associated with acquired neuroprotection and memory formation has been characterized previously both *in vitro* and *in vivo* (Mauceri et al., 2011; Limbäck-Stokin et al., 2004; Zhang et al., 2007; Zhang et al., 2009). The rAAV vectors used contain an expression cassette that harbors a promoter fragment derived from the CaMKIIα promoter and drive expression of mCherry (rAAV-*mCherry*) or mCherry fused to either CaMBP4 (rAAV-*CaMBP4*) (Fig. 1A) or to the inactive CaMBP4 mutant, CaMBP4mu (rAAV-*CaMBP4mu*). To preferentially infect neurons, the neurotropic chimaeric serotype 1/2 was used (During et al., 2003).

We have previously demonstrated that stereotaxic injection of rAAVs (serotype 1/2) directly into the spinal parenchyma enables stable and long-lasting gene delivery with a high rate of gene transduction without inducing any signs of persistent inflammation, injury, gliosis or scar formation (Tappe-Theodor et al., 2007). By mapping the cellular expression patterns of mCherry-tagged CaMBP4 (CaMBP4-mCherry) and mCherry as the prototypes for the different virally expressed proteins used in this study, we found that viral-mediated expression was largely limited to the spinal dorsal horn and, owing to the incorporation of a nuclear localization signal in the expression constructs, was restricted to cell nuclei (Supplementary Fig. 1A).

Co-immunostaining for the neuronal marker NeuN demonstrated a more than 90% co-localization with mCherry or mCherry-tagged CaMBP4 in the superficial spinal laminae (Fig 1B and supplementary Fig. 1B; quantification in Fig. 1C), but not with GFAP, an astrocytic marker or with Iba1, a microglial marker (Fig 1B and supplementary Fig 1B). Using indicator mice that express EGFP in the cell bodies of either glycinergic inhibitory neurons (GlyT2-EGFP) or GABAergic inhibitory interneurons (GAD67-EGFP), we observed that only a small proportion (6–7%) of inhibitory glycinergic or GABAergic interneurons expressed CaMBP4 or mCherry in the spinal dorsal horn (typical examples in Fig. 1D; quantitative analysis in Fig. 1E). Expression in the spinal dorsal horn was evident throughout the spinal segments L2-S1, but reached its maximum in L3–L5, which innervate the hindpaw (supplementary Fig. 1C).

Nociceptive-like synaptic activity induces calcium transients in neuronal nuclei of the spinal dorsal horn

Although it has been suggested that synaptic activity-induced calcium signals can be transduced to the cell soma and invade the cell nucleus, for example in hippocampal neurons (Hardingham, et al. 2001), only recently has it become possible to unambiguously detect calcium transients in the nuclear compartment using genetically-encoded calcium indicators

targeted specifically to cell nuclei (Bengtson, et al. 2010). We used rAAVs to express the calcium sensors GCaMP2.NLS (Bengtson, et al. 2010) or TnXXL.NLS, which are targeted to the nucleus via a tripartite nuclear localization signal at their C-termini, in excitatory neurons of the L3–L5 lumbar spinal cord (Fig. 1F). In acute transverse slices from mice injected with rAAV-*GCaMP2.NLS* (Supplementary Fig. 2A), electrical stimulation of dorsal roots through a suction electrode (20–100 Hz, 0.4–2.0 mA) induced fluorescence intensity changes (Fig. 1G), which corresponded with nuclear calcium transients with a steep rise and slower decay, and that returned to near baseline values within 10 s of stimulus conclusion (traces in Fig 1H). The amplitudes of evoked nuclear calcium transients varied positively with both stimulus intensity (0.4–2.0 mA) (Fig. 1I, J) and frequency (20–100 Hz) (for example, transients at 0.8 mA stimulation intensity are shown in Fig. 1K). These data indicate that robust nuclear calcium responses in nociceptive spinal neurons can be evoked through repetitive stimulation – an activity pattern that may accompany a persistent nociceptive stimulus following injury - as well as by the recruitment of nociceptive C-fiber afferents, which occurs predominantly at higher stimulation intensities (Torsney and MacDermott 2006).

Similar results were obtained when we employed a nuclearly targeted FRET-based calcium indicator, TnXXL.NLS, which by virtue of being a ratiometric, is expected to deliver more consistent responses across experimental preparations independently of expression levels. The amplitudes of evoked nuclear calcium transients (supplementary Fig. 2D) varied positively with both stimulus intensity (supplementary Fig. 2E, F) and frequency (supplementary Fig. 2G). When imaging was performed 24h after bilateral plantar injection of complete Freund's adjuvant (CFA) or PBS (control), we found no detectable differences in the amplitudes of nuclear calcium transients in spinal neurons between CFA-treated and PBS-treated animals, regardless of the stimulation intensity (0.2–3.0 mA) or frequency (1–100 Hz) used (supplementary Fig. 2E–G).

Impact of the blockade of nuclear calcium signaling on behavioral correlates of nociception and inflammatory pain

Using a dynamic aesthesiometer to measure mechanical sensitivity and a plantar test device to study responses to sensitivity to infrared heat, we observed that basal pain sensitivity was similar in mice expressing CaMBP4-mCherry (hereafter referred to simply as CaMBP4) or mCherry (control) in the spinal dorsal horn (Fig. 2A and 2B). CaMBP4 expression did, however, significantly impair the development of mechanical and thermal hypersensitivity following the induction of unilateral hind paw inflammation with CFA. Following CFA-induced inflammation, mCherry-expressing mice showed markedly reduced response latencies to thermal stimulation compared to baseline (black circles in Fig. 2C; $P < 0.05$, ANOVA). This thermal hypersensitivity lasted for up to 7 days following CFA injection. In contrast, CFA-induced inflammation did not significantly alter thermal latency in rAAV-*CaMBP4*-injected animals (red squares in Fig. 2C). Similarly, the development of mechanical hypersensitivity, evident as a decrease in the mechanical response threshold over baseline, occurred prominently in rAAV-*mCherry*-injected mice, but only to a minor extent in rAAV-*CaMBP4*-injected animals (Fig. 2D) throughout the time course of CFA-induced inflammation (up to 10 d; $P < 0.05$, ANOVA). In these experiments, graded von Frey hairs (0.07 – 4g) were applied to the plantar surface and withdrawal threshold was determined as the von Frey filament at which the animal withdrew its paw at least three times out of 8 applications, normalizing basal (pre-CFA) values to 100%. The drop in withdrawal threshold was significantly less pronounced in mice expressing CaMBP4 as compared to mice expressing mCherry (Fig. 2D). To comprehensively present all data on response frequencies to graded von Frey hairs over all forces tested, we constructed a response frequency vs. stimulus intensity (i.e. von Frey force applied) curve per group for every time

point tested and calculated Area under curve (AUC), which was markedly lower in CaMBP4-expressing mice than in mCherry-expressing mice (Fig. 2E). Importantly, mice expressing an inactive mutant of CaMBP4 (CaMBP4mu) exhibited normal levels of thermal and mechanical hyperalgesia (Fig. 2C–E), indicating that the altered nociceptive sensitivity in CaMBP4-expressing mice can be attributed to the functional properties of CaMBP4.

Role of a nuclear calcium effector, CaMKIV, in spinal nociceptive sensitization

Amongst the various signaling events triggered by nuclear calcium/calmodulin, CaMKIV, is particularly importance for gene regulation (Kotera et al., 2005; Racioppi and Means, 2008). To address whether CaMKIV signaling contributes to the observed phenotypic profile of nuclear calcium signaling manipulation, we used a kinase-dead, dominant-negative mutant version of CaMKIV (CaMKIVK75E (Anderson et al., 1997; Mauceri et al., 2011; Zhang et al., 2009). Following rAAV-mediated spinal expression of a FLAG-tagged version of CaMKIVK75E, anti-FLAG immunoreactivity revealed the typical, primarily cytosolic localization of CaMKIVK75E (Chow et al., 2005) over the entire neuronal soma and the neuropil of superficial spinal dorsal horn neurons (Fig. 2F; higher magnification in right hand panel). Following CFA-induced paw inflammation, mice injected into the spinal cord with rAAV-*CaMKIVK75E* initially developed mechanical hypersensitivity to a similar extent as rAAV-*mCherry*-injected mice (Fig. 2G, H), but significantly less mechanical hypersensitivity than the mCherry-expressing group starting from 3 d after injection and, unlike rAAV-*mCherry*-injected mice, recovered baseline mechanical sensitivity within 5 d after injection (Fig. 2G, H). In contrast, CFA-induced thermal hypersensitivity was not markedly affected in rAAV-*CaMKIV75E*-injected mice (Fig. 2I), indicating that particularly the late phase of nuclear calcium-induced mechanical hypersensitivity, but not thermal hypersensitivity, is mediated by activation of CaMKIV in excitatory neurons of the spinal dorsal horn.

Interference with nuclear calcium signaling abrogates nociceptive activity-dependent activation of CREB despite intact ERK1/2 activation

At 24h following CFA-induced peripheral inflammation, serine 133-phosphorylated form of CREB (pCREB) showed increased immunoreactivity in the somata over the entire spinal dorsal horn in rAAV-*mCherry*-injected animals (Fig. 3A) as well as increased expression in immunoblot analyses using lysates of bilaterally-isolated spinal dorsal horns following bilateral intraplantar injection of CFA (Fig. 3B; quantitative analysis from at least 3 experiments in Fig. 3B right panel). In contrast, in mice expressing CaMBP4, paw inflammation failed to increase pCREB immunoreactivity and pCREB expression levels in the spinal dorsal horn (Fig. 3A–B) without any change in basal levels of pCREB immunoreactivity or expression levels of CREB protein in the spinal cord (Fig. 3A–B).

In contrast, after CFA-induced paw inflammation, increased immunoreactivity for the activated, i.e., phosphorylated, forms of ERK1 and ERK2 (pERK1/2) was observed in the neuropil of the superficial spinal dorsal horn in rAAV-*mCherry*-injected mice as well as in rAAV-*CaMBP4*-injected mice (Fig. 3C), which was further confirmed by immunoblot analysis (Fig. 3D). These results indicate an absence of compensatory changes in parallel modes of synapse-to-nucleus communication following specific perturbation of nuclear calcium signaling in the spinal dorsal horn.

Upon induction of paw inflammation, IEGs, such as *c-fos* and *egr1* as well as critical effector genes of nuclear calcium signaling, such as *camk2a* and (*Ptgs2*) (encoding Cox-2), were found to undergo a biphasic transcriptional response with a rapid and transients induction within the first 1 to 6 h after stimulation, followed by a delayed increase in expression at 24 h (Fig. 3E, F), which matched the functional outcomes (i.e. behavioral

hypersensitivity and structural plasticity) that we analyzed 24 h after induction of nociceptive activity (see below).

Differential regulation of acute or chronic plasticity processes regulated by nuclear calcium signals in the spinal cord

We next investigated the temporal phases over which nuclear calcium-driven plasticity processes are operational. We observed that intraplantar injection of capsaicin in the paw acutely evoked nocifensive behaviors, which range between tens of seconds to a few minutes, to a similar extent in rAAV-*CaMBP4*-injected and rAAV-*mCherry*-injected mice (Fig. 4A). Furthermore, intraplantar formalin- induced acute nociceptive behaviors (phase 1, 0–10 min post-injection) and the development of acute nociceptive hypersensitivity, which is known to depend on plasticity in the central nervous system as well as on-going nociceptor activation (phase 2, 15–60 min) were comparable over rAAV-*CaMBP4*-injected and rAAV-*mCherry*-injected mice (Fig. 4B).

The mouse knee arthritis model, which involves unilateral knee-injection of kaolin and carrageenan, enables the assessment of secondary hyperalgesia at hindpaws ipsilateral and contralateral to the inflamed knee (i.e., distinct dermatomes and contralateral processing) and thereby provides insights into central (spinal) mechanisms of nociceptive plasticity spanning several weeks. Whereas rAAV-*mCherry*-injected mice showed ipsilateral hypersensitivity lasting several weeks and beginning within a few days after induction of knee arthritis, rAAV-*CaMBP4*-injected mice failed to develop hyperalgesia over the entire temporal course of arthritic pain assessment (Fig. 4C, 4D). Similar results were obtained for the contralateral paw hyperalgesia after knee arthritis (Supplementary Fig. 3A, B). These behavioral differences did not result from variations in the magnitude of inflammation, since knee edema as well as infiltration of GR1-immunoreactive macrophages into the synovial membrane (Gangadharan et al., 2011) were comparable in rAAV-*mCherry*-injected and rAAV-*CaMBP4*-injected mice (Supplementary Fig. 3C, 3D). Taken together, the results obtained from the capsaicin, formalin, paw inflammation and knee arthritis models suggest that nuclear signaling-dependent plasticity processes do not become evident until several hours after intense nociceptive activity, and that they can persist for several weeks.

Phase-dependent blockade of inflammatory pain by spinal CaMBP4

To determine the contribution of nuclear calcium signaling to the maintenance of inflammatory hypersensitivity independently of the induction phase, we induced arthritic pain prior to expression of CaMBP4. Following development of mechanical hypersensitivity 36 h after arthritis induction (Fig. 4E), mice were randomly divided into two groups, receiving spinal injection of rAAV-*mCherry* or rAAV-*CaMBP4*. In a pilot experiment, we ascertained that injecting rAAVs in the spinal dorsal horn did not, by itself, affect arthritic hypersensitivity at 2–3 days after surgery. Corresponding to the time course of viral expression (i.e. starting 7 days), rAAV-*CaMBP4*-injected mice showed significantly less mechanical hypersensitivity than did rAAV-*mCherry*-injected mice starting from day 15 onwards after injection ($P < 0.05$, ANOVA) (summary of sensitivity over all mechanical forces is shown in Fig. 4E and responses to a force of 0.07 g shown in Fig. 4F). Despite this difference, CaMBP4-expressing mice exhibited levels of mechanical sensitivity that were significantly greater than baseline with a temporal course similar to that observed in rAAV-*mCherry*-injected mice (Fig. 4E, 4F); the partial reduction is likely attributed to spinal plasticity downstream of on-going afferent input coming in from the arthritic knee. These results suggest that spinal nuclear calcium signaling plays a more decisive role in the induction phase than it does in the maintenance phase of nociceptive hypersensitivity.

Profiling genes regulated by nuclear calcium signaling in spinal neurons during inflammatory pain

A genome-wide gene profiling in the CFA model of inflammatory pain was used to identify genes regulated by persistent nociceptive activity in spinal neurons, and to identify the gene pool that is specifically regulated by nuclear calcium signaling. cDNA prepared from spinal dorsal horn tissue 24 h after bilateral intraplantar paw injection of CFA (inflamed) in rAAV-*mCherry* or rAAV-*CaMBP4*-injected mice was used for microarray-based transcriptome analysis, and the degree of induction or repression over basal state (control) was analyzed.

We found 3165 genes to be up-regulated and 5143 genes to be down-regulated with a P value ≤ 0.050 in inflamed versus control samples derived from rAAV-mCherry-injected mice (t-tests with Benjamini-Hochberg correction for multiple comparisons). To narrow down the gene pool for subsequent detailed analyses, we set a cut-off of 1.40-fold for up-regulated genes and of 0.70-fold for down-regulated genes in mCherry-expressing mice and assessed how CaMBP4 expression influenced the inflammation-induced up-regulation or down-regulation of each of these selected genes (Fig. 5A–D). All genes regulated in nuclear calcium-dependent manner by the criteria used (see methods) are listed in Supplementary Table 1. The complete profiling data is shown in Supplementary Table 2. Individual up-regulated or down-regulated genes are schematically represented at the same position in Figure 5 (panels A, B and C, D). Of the 202 genes up-regulated at least 1.40-fold following CFA injection in mCherry-expressing mice, 127 genes (i.e., 63%) were not induced by CFA by at least 1.40-fold in CaMBP4-expressing mice (Supplementary Table 1); these genes were categorized as ‘100% inhibition of induction by CaMBP4’ (see methods for details) and marked as dark blue fields in Fig. 5B (detailed information on % difference in fold-induction is provided in Supplementary Table 2). The induction of 26 genes was inhibited by at least 20% and that of many more genes was inhibited by between 10 and 20% (indicated by fields in graded shades of blue in Fig. 5B). Of the 288 genes repressed by CFA by at least 0.70-fold in mCherry-expressing mice, 164 genes (i.e., 57%) were not repressed by at least 0.7-fold by peripheral inflammation in CaMBP4-expressing mice (Supplementary Table 1); they were categorized as ‘100% inhibition of repression by CaMBP4’ (see methods for details) and marked as dark blue fields in Fig. 6D (detailed information on % difference in fold-repression is provided in Supplementary Table 2). The down-regulation of another 34 genes was inhibited by at least 20% (blue shaded fields in Fig. 5D) (Supplementary table 1). A small number of genes that was repressed or induced by paw inflammation in rAAV-*mCherry*-injected mice was found to be repressed or induced to a greater extent in rAAV-*CaMBP4*-injected mice (6.6% and 5% respectively), suggesting that nuclear calcium signaling serves to counteract an endogenous mechanism involved in the repression of these genes by paw inflammation (yellow and brown-shaded fields Fig. 5D) (Supplementary Table 1). About 28% of all genes regulated within the above-mentioned cut-off in a nuclear calcium-dependent manner in the spinal dorsal horn represent known or putative targets of CREB as predicted by the CREB Target Gene Database (Salk Institute). Importantly, we also observed that the regulation of a subset of genes by paw inflammation was not significantly affected by the blockade of nuclear calcium signaling: about 10% of genes up-regulated by at least 1.4-fold and 19% of genes down-regulated by at least 0.7-fold in mCherry-expressing mice exhibited similar levels of regulation by paw inflammation in CaMBP4-expressing mice (white fields in Fig. 5B and 5D, respectively).

The validity of the transcriptome data was confirmed by quantitative reverse transcriptase-polymerase chain reaction (QRT-PCR) analysis; one example, *grip1*, a gene encoding the key postsynaptic protein GRIP1 at excitatory synapses (Dong et al., 1997), is shown in Fig. 5E. As expected from previous profiling analyses (e.g. Zhang et al., 2007; Zhang et al., 2009), the level of regulation determined by QRT-PCR analysis was much higher than that observed in the gene chip-based assessment. Whereas CaMBP4 expression suppressed gene

expression of some genes in both basal and inflammatory states,, e.g. the genes encoding Tachykinin1 (*Tac1*) and Cholecystokinin (*Cck*) (Fig. 5E), expression of others was only suppressed in inflamed mice, e.g. *Gucy1a2*, which encodes soluble guanylate cyclase 1 (Fig. 5E).

Nuclear calcium mediates activity-induced regulation of a large set of pain-relevant genes

Amongst the genes that were significantly regulated by paw inflammation ($P < 0.05$) in a nuclear calcium-dependent manner using the criteria mentioned above, we found a large number of genes encoding proteins that have been implicated in the positive or negative modulation of nociception. We chose Cox-2 (*Ptgs2*) as an example of a prominent pain target (Vardeh et al., 2009) and found that its regulation by nuclear calcium signaling both in the spinal dorsal horn (Fig. 5F) and, as shown previously (Zhang et al., 2009), in hippocampal neurons. Mice spinally injected with rAAVs to express a Cox-2 specific short hairpin RNA (shRNA) showed lower levels of Cox-2-induction 24 h after paw inflammation than mice expressing a control shRNA (Fig. 5F), although due to expression of Cox-2 in glial cells (Vardeh et al., 2009) that are not targeted by the rAAV, significant amounts of Cox-2 mRNA could still be detected in the spinal cord. The selective knock-down of Cox-2 expression in spinal excitatory neurons resulted in a failure of the animals to develop mechanical hypersensitivity following paw inflammation (Fig. 5G), but no change in CFA-induced thermal hypersensitivity was observed (Fig. 5H).

Interestingly, our profiling results indicate marked differences in gene programs associated with inflammatory and neuropathic pain states. For example, genes encoding P_2X_4, MMP-2, and cathepsin S, which are upregulated in neuropathic pain states (Gao and Ji, 2010) were observed to be downregulated in spinal dorsal horn samples of inflamed mice after CFA using QRT-PCR (Fig. 6A). Conversely, we found that genes including *egr1*, *Ptgs2* and *c-fos*, which were upregulated in inflamed mice in our profiling analyses (Fig. 3E, F & Fig. 5E), are downregulated at 7 days after the induction of spared nerve injury (SNI), a model of neuropathic pain (Fig. 6B). In the SNI model of neuropathic pain, mCherry- or CaMBP4-injected mice showed a similar drop in response threshold to von Frey stimuli over basal values (calculated as a force eliciting a miminum of 40% response frequency to 5 applications of each von Frey hair) (Fig. 6C). When stimulus intensity-response frequency analyses were compared for all von Frey forces tested by calculating the area under the curve (AUC), only a small, but statistically significant, decrease in the extent of SNI-induced mechanical hypersensitivity was observed in CaMBP4-injected mice compared to mCherry-injected mice (Fig. 6D), which can also be attributed to on-going inflammation at the nerve injury site. This indicates differences in the requirement of nuclear calcium signaling in spinal excitatory neurons in inflammatory and neuropathic pain processes.

Bioinformatics analysis of new genes and pathways in spinal pain processing

We subjected 421 putative targets of nuclear calcium signaling in spinal dorsal horn neurons in inflammatory pain that were identified by the criteria used (Supplementary Table 1) to further bioinformatics analysis of putative molecular ontology, pathways and function using the bioCompendium database of the European Molecular Biology Laboratory (http://biocompendium.embl.de). The best-represented functional ontologies in our group of regulated genes corresponded to protein-binding activities, of which about a quarter show binding to cytoskeletal elements. Amongst the genes encoding receptor molecules, the largest fraction was represented by GPCRs, followed by tyrosine kinase receptors, cytokine receptors, glutamate receptors, GABA-A receptors and surprisingly, receptors of the immunoglobulin families. Finally, about 4% of the nuclear calcium target genes in the spinal dorsal horn were kinases, in particular protein tyrosine and threonine/serine kinases,

including members of the MAP kinase and the calcium/calmodulin-dependent kinase family, as well as the lipid kinase, di-acyl glycerol kinase.

In a second step, we performed a network analysis using the MetaCore database (Ekins et al., 2007) on genes chosen from profiling data. For example, a birds-eye view of the interactions between all genes, which are up-regulated is provided in Supplementary Fig. 4. Within these interactions, we found a number of genes to be clustered in highly connected networks, which are indicated by an arrow in Supplementary Fig. 4A, and are shown at a higher magnification in Supplementary Fig. 4B. Transcription factors (TFs) such as STAT-3 and STAT-1 (Supplmentary Fig. 4B) were found to serve as key nodal points in interaction maps of the nuclear calcium-regulated gene pool, potentially implicating these TFs as key to the cellular response to nuclear calcium signaling.

Identification of a novel nuclear calcium target and its functional validation as a modulator of inflammatory pain

Two distinct prediction algorithms for pathway analysis (Ingenuity Systems and MetaCore; Ekins et al., 2007) independently suggested ‘Immune response classical complement pathway’ as the most significantly altered pathway in the spinal dorsal horn following peripheral inflammation. In profiling analysis, we found that mCherry-expressing mice, but not CaMBP4 expressing mice, showed a significant down-regulation of genes encoding the complement proteins, such as the initiator of the complement cascade C1q (including all 3 members of the active complex) as well as C1, C3a, C4a, C4b and C3 convertase in the spinal cord after paw inflammation. QRT-PCR analysis for one member of the trimeric complex, C1q-c in CaMBP4-expressing mice, not only confirmed that nuclear calcium signaling in spinal neurons mediates nociception-induced down-regulation of C1q, but also indicated that it also suppresses a pathway involved in sustaining basal C1q expression levels in the spinal neurons (Fig. 7A).

An up-regulation of complement proteins, including C1q, has been observed in spinal microglia after nerve injury, which is consistent with our observation of *C1q-c* upregulation in spinal cord of neuropathic mice (Fig. 7A), and has been associated with the activation and proliferation of microglia in the spinal cord (Griffin et al., 2007). This mechanism did not appear likely in the our experimental paradigms, given that we observe a down-regulation of C1q after paw inflammation and that molecular perturbations applied in this study were restricted to neurons (above; During et al. 2003)(Fig. 1 & supplementary Fig. 1). Furthermore, consistent with previous reports (e.g. Lin et al., 2007), we did not observe an overt spinal microglial activation as assayed by Iba1 immunoreactivity in inflamed mice (Fig. 7B; supplementary Fig. 5A), in contrast to neuropathic mice (supplementary Fig. 5C). Furthermore, intrathecal application of C1q to mice with paw inflammation did not induce microglia proliferation or recruitment (Fig. 7C; supplementary Fig. 5B).

Inspired by recent studies implicating C1q-like proteins, which resemble C1q in structure and functional motifs, in synaptic morphogenesis during brain development (Chu et al., 2010; Fourgeaud and Boulanger, 2010), we investigated whether C1q can modulate synaptic contacts on mature excitatory neurons of the spinal cord. Dissociated neonatal mouse spinal cord cultures matured over 4 weeks *in vitro* were infected with an rAAV-*CaMKII-EGFP* construct enabling visualization of the dendritic trees and synaptic spines in virus-targeted excitatory neurons. A significant reduction of the density of EGFP-labeled dendritic synaptic spines was observed upon a single application of C1q, but not vehicle alone, to mature cultures within 24 h, which was even more pronounced at 96 h (typical examples in Fig. 7D; a quantitative analysis in Fig. 7E). C1q application did not evoke signs of nuclear damage or cell death in neurons (data not shown). Spinal expression of rAAVs expressing shRNAs against *C1q-c* (validation in neurons via QRT-PCR is shown in Fig. 7F), led to a

small, but significant, increase in spine number on dendrites of cultured spinal neurons (Fig. 7G).

Similar to the results obtained with spinal cord neurons, expression of CaMBP4 in hippocampal neurons led to an increase in *C1q-c* expression, confirming *C1q-c* as a nuclear calcium-regulated gene (Fig. 7H). Application of recombinant C1q markedly reduced spine density on hippocampal neurons (Fig. 7I, quantification in 7J). However, in contrast to spinal neurons, we did not detect a significant effect of the knockdown of C1q-c via shRNA on the spine density of hippocampal neurons (Fig. 7J).

We next investigated the role of C1q as a possible modulator of synaptic spine density *in vivo* by performing Golgi staining on spinal cords derived from mice 24 h after intraplantar paw injection of CFA or PBS (Fig. 8A). Because the very superficial dorsal horn neurons displayed less sensitivity to impregnation, we restricted our analysis to lamina II neurons and mostly to large pyramidal lamina V neurons. These showed a marked increase in spine density on primary and secondary dendrites in inflamed mice as compared to control mice (examples in Fig. 8B, higher magnification in Fig. 8C and quantification in Fig. 8D). Mice injected spinally with rAAV-*C1q-c-shRNA-GFP* showed an increase in spine density on spinal neurons as compared to rAAV-*scrambled-shRNA-GFP*-injected mice (Fig. 8C, 8F). In contrast, following intrathecal application of recombinant C1q in inflamed mice, CFA-associated increase in spine density was significantly reduced (Fig. 8C, 8D). Similarly, following stereotaxic *in vivo* injection of C1q in the hippocampus of adult mice, a significant reduction in spine density in pyramidal neurons of CA1 region was observed (Fig. 8E).

Finally, nuclear calcium-evoked spinal C1q downregulation was simulated by injection of rAAV-*C1q-c-shRNA-GFP* (using rAAV-scrambled-RNA as a control) into the spinal dorsal horn; whereas basal mechanical sensitivity was largely unaltered upon spinal C1q knockdown, the extent of inflammatory mechanical hypersensitivity was significantly increased as compared to mice expressing scrambled control RNA (Fig. 8G and supplementary Fig. 7A, B). Conversely, when we intrathecally applied recombinant trimeric C1q, significant attenuation of CFA-induced mechanical and thermal hypersensitivity was observed (Fig. 8H, I and supplementary Fig. 7C, D; $P < 0.05$, ANOVA) without any change in basal thermal and mechanical sensitivity in the absence of inflammation (Supplementary Fig. 8A–D). Taken together with the morphological data, these experiments provide evidence for a novel nuclear calcium target gene in the modulation of inflammation-associated pain hypersensitivity as well as structural plasticity.

Discussion

The interplay between synaptic receptors, cytoplasmic effectors and the nucleus plays a critical role in linking membrane depolarization to gene transcription. Here we show that high threshold, persistent nociceptive input leads to calcium entry into the nuclei of spinal dorsal horn neurons, which exhibit a specific transcriptional response drives structural remodelling in spinal excitatory neurons and functional changes, leading to chronic inflammatory hypersensitivity.

We observed that progressively augmenting recruitment of A-delta afferents and C-type nociceptors as well as stimulating nociceptors with increasing frequencies led to progressive rise in the amplitude of activity evoked-nuclear calcium signals, suggesting that nuclear calcium integrates spinal neuron input from persistent activation of nociceptors after injury. Interestingly, using constant stimulation parameters in naïve or CFA-inflamed mice, we found no detectable differences in the characteristics of evoked nuclear calcium signals,

consistent with the concept that nuclear calcium transients are upstream, not downstream, of activity-induced plasticity. These data are consistent with the observed specific role for CaMBP4 in markedly attenuating inflammatory hypersensitivity triggered repetitive activation of nociceptors without affecting basal and acute nociceptive responses evoked by an acute activation of nociceptors. These findings, taken together with the results of experiments addressing the temporal profile of the impact of blockade nuclear calcium signaling on nociceptive hypersensitivity, indicate that a genomic program governed by nuclear calcium signaling in spinal neurons plays a major role in the induction of long-lasting nociceptive hypersensitivity following persistent nociceptive activity, but not in its maintenance.

Nociceptive activity-induced phosphorylation of CREB has been reported in models of inflammatory and neuropathic pain (Ji and Rupp, 1997). CaMKII activity as well as protein kinases PKA, PKC and ERK1/2 have been implicated in CREB phosphorylation in spinal nociceptive neurons (Kawasaki et al., 2004; Wang et al., 2011). We observed that blocking nuclear calcium signaling in spinal excitatory neurons blocked nociceptive activity-driven phosphorylation of CREB albeit ERK1/2 were activated normally, indicating that other synapse-to-nucleus messengers are not sufficient for activating CREB in spinal neurons in the absence of nuclear calcium signaling. These findings together with the observation that inflammatory hypersensitivity was attenuated by inhibiting CaMKIV activity indicate that nuclear calcium-CaMKIV-CREB/CBP signaling is the primary mediator of long-term nociceptive sensitization.

Whole genome expression array analysis indicated that the transcriptional program controlled by nuclear calcium in spinal nociceptive neurons spans a wide range of genes, including key modulators of nociceptive processing and neuronal excitation. These include several ion-channels such as the beta4 subunits of voltage-dependent calcium channels, GABA-A channel subunits, the alpha2/delta3 variant of voltage-dependent calcium channels, which was recently identified as an evolutionarily conserved pain gene regulating noxious heat pain from drosophila to humans (Neely et al., 2010), amongst others. Interestingly, spinal nuclear calcium targets spanned several key components of the cellular machinery involved in promoting AMPA receptor (AMPAR)-mediated transmission at spinal synapses, e.g., CaMKIIα, GRIP1, which play a key role in potentiating synapses, unsilencing synapses, and the development of nociceptive hypersensitivity *in vivo* (Li et al., 1999; Fang et al., 2004). Several of the spinal nuclear calcium-regulated genes are directly or indirectly involved in spinal long-term potentiation (LTP) mechanisms (Sandkühler, 2009), consistent with our observation that LTP paradigms yield the highest magnitudes of nuclear calcium transients in spinal neurons. Nuclear calcium signaling is involved in the transition from early-LTP to late-LTP in hippocampal pyramidal neurons (Bengston et al. 2010), indicating a scope for nuclear calcium signaling in facilitation and amplification of peripheral nociceptive information passing through the spinal cord on its way to the brain. Additional nuclear calcium targets included several key pain-relevant GPCRs, GASP1, a protein which critically regulates trafficking and lysosomal sorting of GPCRs and thereby mediates drug tolerance to GPCR ligands (Tappe-Theodor et al., 2007) as well as diverse chemokines, diverse cathepsins, matrix metalloproteases that have been implicated in synaptic modulation and neuron-glia communication (Kawasaki et al., 2008, Gao and Ji 2004).

An important advantage of the combined approach of cell-specific molecular perturbations, genome-wide profiling and detailed bioinformatics analyses employed here was that it opened possibilities for discovering novel mediators of plasticity governed by nuclear calcium, which could thereby offer unprecedented insights into mechanisms of persistent pain. Amongst the novel mediators found *in silico*, we focused on the complement system,

which we identified as a prominently modulated pathway in neurons of inflamed mice, different from its previously reported activation in spinal glia of neuropathic mice (Griffin et al. 2007). As described in details under results, our findings suggest a differential and reciprocal modulation of the complement system in microglia and neurons in neuropathic and inflammatory pain states, respectively, and we report that the novel pain-modulatory role for C1q in inflammatory states described here is associated with synapse elimination in spinal neurons in response to afferent activity, rather than microglial modulation, underlies. Because modulation of C1q expression by CaMBP4 as well as shRNAs was restricted to spinal excitatory neurons, which thereupon showed reciprocal changes in spine density, we deduce that spinal excitatory neuronal circuits constitute both, the locus of C1q regulation as well as its action, either in an autocrine or paracrine manner. Interestingly, our analyses on hippocampal neurons indicate that C1q is a common target of nuclear calcium signaling across neuronal types, and taken together with data on the role of C1q-like proteins in developmental synapse pruning in the brain (Chu et al., 2010; Fourgeaud and Boulanger, 2010), appears to function as global regulator of not only developmental spine morphogenesis, but also activity-dependent remodelling. Indeed, by bidirectionally altering C1q expression in spinal neurons and combining this with morphometric and behavioral analyses, we observed a most intriguing and close link between nociceptive activity, C1q expression levels, density of synaptic spines on spinal neurons *in vivo* and the magnitude of inflammatory hypersensitivity. These findings suggest that inflammatory pain involves a concerted and tightly-regulated unfolding of processes underlying structural remodelling and functional plasticity and further, they indicate that nuclear calcium signaling plays a key role in these mechanisms.

In summary, this study places nuclear calcium as a key synapse-to-nucleus messenger system in spinal excitatory neurons. Moreover, it provides evidence that a nuclear calcium-driven genomic program shapes activity-dependent functional plasticity as well as structural remodelling in spinal circuits, thereby amplifying nociceptive sensitivity.

Methods

Virus production and *in vivo* injection

A recombinant adeno-associated virus (rAAV) vector with a AAV1/AAV2 chimeric backbone containing a 1.3 kbp fragment of the mouse CaMKIIα promoter was used to express diverse proteins. Viral particles were produced, purified and injected intrahippocampally as described previously (Zhang et al. 2009, Mauceri et al. 2011). Spinal cord injections of virions ($2–5 \times 10^9$ particles/ml, 500 nl of a 2:1 mixture with 20% Mannitol) in C57BL/6J adult mice was performed as as described previously (Tappe-Theodor et al., 2007) at least 3 weeks after surgery prior to behavioral, morphological or imaging experiments. Please see supplementary methods for details.

Transgenic indicator mice

Mice expressing enhanced green fluorescent protein (EGFP) under the control of the promoter of the glycine transporter 2 (GlyT2) gene were used for identifying glycinergic neurons (a generous gift from H.U. Zeilhofer, Univ. Zürich). Mice expressing EGFP under control of GAD 67 were used for identifying GABAergic neurons (a generous gift from H. Monyer, Univ. Heidelberg).

Calcium imaging

Lumbar spinal slices with attached dorsal roots were derived from virally-injected mice as described in details previously (Luo et al., 2008). Dorsal roots were stimulated with 1s trains (1–100 Hz) of 0.2–3.0 mA square electrical pulses lasting 0.2 ms and Ca^{2+} responses

elicited were imaged as described in details previously (Bengston et al. 2010). See supplementary methods for further details.

Behavioral testing of nociception and pathological nociceptive sensitivity

All animal use procedures were in accordance with ethical guidelines imposed by the local governing body (Regierungspräsidium Karlsruhe, Germany) and involved mice aged 8–16 weeks and matched for gender and age. Inflammation of the paw or knees (arthritis) was induced by subcutaneous plantar injection of 20 μl Complete Freund's Adjuvant (CFA, Sigma) or 4% Kaolin (Sigma, K7375) with 2% Carrageenan Lambda (Sigma, C-3889) under isoflurane anesthesia subcutaneously as described previously (Gangadharan et al. 2011). The Spared nerve injury (SNI) model of neuropathic pain was employed ligating and severing common peroneal and tibial branches of the left sciatic nerve. Behavioral testing was carried out in habituated mice by an observer blinded to the identity of the groups. Mechanical sensitivity was determined upon paw withdrawal to either application of graded force via a dynamic aesthesiometer (UgoBaile Inc.) or to manual application of graded von Frey hairs (0.008–4 g) to the plantar surface (Gangadharan et al. 2011). To determine thermal sensitivity, paw withdrawal latency to a ramp of infrared heat was measured using a plantar test apparatus (Ugo Basile Inc.). Formalin (1%, 20 μl) or Capsaicin (0.03%, 20 μl) was injected into the plantar surface of the hindpaw and the duration of nocifensive behaviors (lifting, licking, or flinching) was measured over 60 min or 5 min, respectively, post-injection (Gangadharan et al. 2011). Additional details are given in Supplementary materials.

Antibodies used for Western blotting or immunohistochemistry

The following antibodies were used in dilutions in 5% normal horse serum in PBS for immunohistohemistry: monoclonal rabbit anti-pCREB und anti-pERK (Cell Signaling) 1:100, monoclonal mouse anti-NeuN: 1:500 (Millipore), monoclonal rabbit anti-GFAP 1:500 (DAKO), polyclonal goat anti-Iba-1: 1:150 (Abcam) and a rabbit Anti-Flag-M2 AB 1:1000 (Sigma), appropriate FITC-conjugated secondary antibodies, anti-Fos antibody (Rabbit anti-c-Fos Ab-5 1:20000, Merck) followed by biotinylated secondary anti-rabbit antibody (1:200). Rabbit anti- P-CREB, anti-P-ERK1/2, anti-CREB and anti-ERK1/2 (all from Cell Signaling Inc.) antibodies were used for Western blotting at 1:1000 in 5% BSA in TBST overnight followed by anti-rabbit HRP-conjugated antibody (1:2000). See supplementary methods for further details.

Neuronal cultures and analysis of spine density

Hippocampal neurons from newborn C57BL/6J mice were cultured and was transfected with a plasmid encoding hrGFP on DIV8 using Lipofectamine 2000 as described (Mauceri et al. 2011). Spinal cord cultures derived from mouse embryos at embryonic day E16 were infected with AAV-CaMKIIα-EGFP virions at P7, fixed 4 weeks later and examined with a laser-scanning confocal microscope (Leica SP2 AOBS) using a 100x objective (Leica). To analyse dendritic spines *in vivo*, Golgi–Cox staining was performed using an FD Rapid GolgiStain Kit (FD Neurotechnologies, Ellicott, MD) as described in details in Mauceri et al., 2011. See details under supplementary methods.

Quantitative RT-PCR

Quantitative RT-PCR (QRT-PCR) was performed using TaqMan Universal PCR Master Mix with a sequence detection system model 7300 Real Time PCR System (Applied Biosystems, Foster City, California, USA) with the following FAM dye-labeled TaqMan MGB probes. See supplementary methods for further details.

Statistics

All data are expressed as mean ± standard error of the mean (S.E.M.). In behavioral, morphological and RT-PCR analysis, two-tailed unpaired student's t-test or one-way ANOVA with post-hoc Dunnett's or Fisher's tests were used. t-tests with Benjamini-Hochberg correction for multiple comparisons Changes with $p < 0.05$ were considered to be significant.

Gene profiling and bioinformatics analysis

cDNA samples for gene profiling analysis were prepared as described in Zhang et al. 2009 and analyzed as described under supplementary methods in detail. While representing genes regulated by CFA inflammation over the naïve state in mCherry-injected mice (i.e. controls), a cut-off of 1.4 was applied for upregulated genes and a cut-off of 0.7 was applied for downregulated genes. In order to assess how CFA-induced up- or downregulation of genes was affected by interfering with nuclear calcium signaling in spinal neurons, fold regulation (i.e. CFA over naïve) was compared between mCherry-injected mice and CaMBP4-injected mice. The percent change in down- or up-regulation was calculated for all genes for which CaMBP4 fold-changes were <= 0.70 or >= 1.40 using the following formula: 100% * [(CaMBP4 − 1) − (mCherry − 1)]/(mCherry − 1). For genes for which CaMBP4 fold-changes were > 0.70 or < 1.40, the percent change in down- or up-regulation was set at 100%. Gene Ontology (GO) analysis was performed on regulated genes using a Perl program 'map2slim' from 'go-perl' (http://search.cpan.org/~cmungall/go-perl/go-perl.pod) as described in details under supplementary methods. Network analysis and visualization and pathway analysis were performed using MetaCore (www.genego.com; Ekins et al., 2007) as described in details under supplementary methods.

Supplementary Material

Refer to Web version on PubMed Central for supplementary material.

Acknowledgments

The authors are grateful to Rose LeFaucheur for secretarial assistance and to Hans-Joseph Wrede, Karin Meyer and Dunja Baumgartl-Ahlert for technical assistance. This work was supported by grants from the Deutsche Forschungsgemeinschaft to RK and HB and ERC Advanced Grants to RK and HB. DV was supported by a fellowship from the Postdoctoral College financed by the Medical Faculty of Heidelberg University. MC thanks the US National Institutes of Health for their support (R01-NS074430-01A1). RK and HB are principal investigators in the Excellence Cluster 'CellNetworks' of Heidelberg University and MS and AMH were supported by the CellNetworks Postdoctoral Fellowship program.

References

Bengtson CP, Freitag HE, Weislogel JM, Bading H. Nuclear calcium sensors reveal that repetition of trains of synaptic stimuli boosts nuclear calcium signaling in CA1 pyramidal neurons. Biophysical journal. 2010; 99:4066–4077. [PubMed: 21156150]

Buchthal B, Lau D, Weiss U, Weislogel JM, Bading H. Nuclear Calcium Signaling controls Methyl-CpG-binding Protein 2 (MeCP2) Phosphorylation on Serine 421 following Synaptic Activity. The Journal of biological chemistry. 2012; 287:30967–30974. [PubMed: 22822052]

Chow FA, Anderson KA, Noeldner PK, Means AR. The autonomous activity of calcium/calmodulin-dependent protein kinase IV is required for its role in transcription. The Journal of biological chemistry. 2005; 280:20530–20538. [PubMed: 15769749]

Chu Y, Jin X, Parada I, Pesic A, Stevens B, Barres B, Prince DA. Enhanced synaptic connectivity and epilepsy in C1q knockout mice. Proceedings of the National Academy of Sciences of the United States of America. 2010; 107:7975–7980. [PubMed: 20375278]

During MJ, Young D, Baer K, Lawlor P, Klugmann M. Development and optimization of adeno-associated virus vector transfer into the central nervous system. Methods in molecular medicine. 2003; 76:221–236. [PubMed: 12526166]

Ekins S, Nikolsky Y, Bugrim A, Kirillov E, Nikolskaya T. Pathway mapping tools for analysis of high content data. Methods in molecular biology. 2007; 356:319–350. [PubMed: 16988414]

Fang L, Wu J, Lin Q, Willis WD. Calcium-calmodulin-dependent protein kinase II contributes to spinal cord central sensitization. J Neurosci. 2002; 22:4196–4204. [PubMed: 12019337]

Fourgeaud L, Boulanger LM. Role of immune molecules in the establishment and plasticity of glutamatergic synapses. The European journal of neuroscience. 2010; 32:207–217. [PubMed: 20946111]

Gangadharan V, Wang R, Ulzhofer B, Luo C, Bardoni R, Bali KK, Agarwal N, Tegeder I, Hildebrandt U, Nagy GG, et al. Peripheral calcium-permeable AMPA receptors regulate chronic inflammatory pain in mice. The Journal of clinical investigation. 2011; 121:1608–1623. [PubMed: 21383497]

Gao YJ, Ji RR. Chemokines, neuronal-glial interactions, and central processing of neuropathic pain. Pharmacol Ther. 2010; 126:56–68. [PubMed: 20117131]

Geranton SM, Morenilla-Palao C, Hunt SP. A role for transcriptional repressor methyl-CpG-binding protein 2 and plasticity-related gene serum- and glucocorticoid-inducible kinase 1 in the induction of inflammatory pain states. J Neurosci. 2007; 27:6163–6173. [PubMed: 17553988]

Griffin RS, Costigan M, Brenner GJ, Ma CH, Scholz J, Moss A, Allchorne AJ, Stahl GL, Woolf CJ. Complement induction in spinal cord microglia results in anaphylatoxin C5a-mediated pain hypersensitivity. J Neurosci. 2007; 27:8699–8708. [PubMed: 17687047]

Hagenston AM, Bading H. Calcium Signaling in Synapse-to-Nucleus Communication. Cold Spring Harbor perspectives in biology. 2011; 3

Hardingham GE, Chawla S, Johnson CM, Bading H. Distinct functions of nuclear and cytoplasmic calcium in the control of gene expression. Nature. 1997; 385:260–265. [PubMed: 9000075]

Hardingham GE, Arnold FJ, Bading H. Nuclear calcium signaling controls CREB-mediated gene expression triggered by synaptic activity. Nature neuroscience. 2001; 4:261–267.

Impey S, McCorkle SR, Cha-Molstad H, Dwyer JM, Yochum GS, Boss JM, McWeeney S, Dunn JJ, Mandel G, Goodman RH. Defining the CREB regulon: a genome-wide analysis of transcription factor regulatory regions. Cell. 2004; 119:1041–1054. [PubMed: 15620361]

Ji RR, Rupp F. Phosphorylation of transcription factor CREB in rat spinal cord after formalin-induced hyperalgesia: relationship to c-fos induction. J Neurosci. 1997; 17:1776–85. [PubMed: 9030636]

Ji RR, Baba H, Brenner GJ, Woolf CJ. Nociceptive-specific activation of ERK in spinal neurons contributes to pain hypersensitivity. Nature neuroscience. 1999; 2:1114–1119.

Kawasaki Y, Kohno T, Zhuang ZY, Brenner GJ, Wang H, Van Der Meer C, Befort K, Woolf CJ, Ji RR. Ionotropic and metabotropic receptors, protein kinase A, protein kinase C, and Src contribute to C-fiber-induced ERK activation and cAMP response element-binding protein phosphorylation in dorsal horn neurons, leading to central sensitization. J Neurosci. 2004; 24:8310–8321. [PubMed: 15385614]

Kotera I, Sekimoto T, Miyamoto Y, Saiwaki T, Nagoshi E, Sakagami H, Kondo H, Yoneda Y. Importin alpha transports CaMKIV to the nucleus without utilizing importin beta. The EMBO journal. 2005; 24:942–951. [PubMed: 15719015]

Kuner R. Central mechanisms of pathological pain. Nature medicine. 2010; 16:1258–1266.

Li P, Kerchner GA, Sala C, Wei F, Huettner JE, Sheng M, Zhuo M. AMPA receptor-PDZ interactions in facilitation of spinal sensory synapses. Nature neuroscience. 1999; 2:972–977.

Limbäck-Stokin K, Korzus E, Nagaoka-Yasuda R, Mayford M. Nuclear calcium/calmodulin regulates memory consolidation. J Neurosci. 2004; 24:10858–10867. [PubMed: 15574736]

Lin T, Li K, Zhang FY, Zhang ZK, Light AR, Fu KY. Dissociation of spinal microglia morphological activation and peripheral inflammation in inflammatory pain models. Journal of neuroimmunology. 2007; 192:40–48. [PubMed: 17919739]

Luo C, Seeburg PH, Sprengel R, Kuner R. Activity-dependent potentiation of calcium signals in spinal sensory networks in inflammatory pain states. Pain. 2008; 140:358–367. [PubMed: 18926636]

Mauceri D, Freitag HE, Oliveira AM, Bengtson CP, Bading H. Nuclear calcium-VEGFD signaling controls maintenance of dendrite arborization necessary for memory formation. Neuron. 2011; 71:117–130. [PubMed: 21745642]

Neely GG, Hess A, Costigan M, Keene AC, Goulas S, Langeslag M, Griffin RS, Belfer I, Dai F, Smith SB. A genome-wide Drosophila screen for heat nociception identifies alpha2delta3 as an evolutionarily conserved pain gene. Cell. 2010; 143:628–638. [PubMed: 21074052]

Oliveira AM, Hemstedt TJ, Bading H. Rescue of aging-associated decline in Dnmt3a2 expression restores cognitive abilities. Nature Neuroscience. 2012; 15:1111–1113.

Racioppi L, Means AR. Calcium/calmodulin-dependent kinase IV in immune and inflammatory responses: novel routes for an ancient traveller. Trends in immunology. 2008; 29:600–607. [PubMed: 18930438]

Restivo L, Tafi E, Ammassari-Teule M, Marie H. Viral-mediated expression of a constitutively active form of CREB in hippocampal neurons increases memory. Hippocampus. 2009; 19:228–234. [PubMed: 19004015]

Sandkühler J. Models and mechanisms of hyperalgesia and allodynia. Physiological reviews. 2009; 89:707–758. [PubMed: 19342617]

Tappe-Theodor A, Agarwal N, Katona I, Rubino T, Martini L, Swiercz J, Mackie K, Monyer H, Parolaro D, Whistler J, et al. A molecular basis of analgesic tolerance to cannabinoids. J Neurosci. 2007; 27:4165–4177. [PubMed: 17428994]

Torsney C, MacDermott AB. Disinhibition opens the gate to pathological pain signaling in superficial neurokinin 1 receptor-expressing neurons in rat spinal cord. J Neurosci. 2006; 26:1833–1843. [PubMed: 16467532]

Vardeh D, Wang D, Costigan M, Lazarus M, Saper CB, Woolf CJ, Fitzgerald GA, Samad TA. COX2 in CNS neural cells mediates mechanical inflammatory pain hypersensitivity in mice. The Journal of clinical investigation. 2009; 119:287–294. [PubMed: 19127021]

Vo N, Goodman RH. CREB-binding protein and p300 in transcriptional regulation. The Journal of biological chemistry. 2001; 276:13505–13508. [PubMed: 11279224]

Wang Y, Cheng X, Xu J, Liu Z, Wan Y, Ma D. Anti-hyperalgesic effect of CaMKII inhibitor is associated with downregulation of phosphorylated CREB in rat spinal cord. Journal of anesthesia. 2011; 25:87–92. [PubMed: 21188428]

Woolf CJ, Costigan M. Transcriptional and posttranslational plasticity and the generation of inflammatory pain. Proceedings of the National Academy of Sciences of the United States of America. 1999; 96:7723–7730. [PubMed: 10393888]

Zhang SJ, Steijaert MN, Lau D, Schutz G, Delucinge-Vivier C, Descombes P, Bading H. Decoding NMDA receptor signaling: identification of genomic programs specifying neuronal survival and death. Neuron. 2007; 53:549–562. [PubMed: 17296556]

Zhang SJ, Zou M, Lu L, Lau D, Ditzel DA, Delucinge-Vivier C, Aso Y, Descombes P, Bading H. Nuclear calcium signaling controls expression of a large gene pool: identification of a gene program for acquired neuroprotection induced by synaptic activity. PLoS genetics. 2009; 5:e1000604. [PubMed: 19680447]

Highlights

- Nociceptive-like signals induce nuclear calcium transients in spinal cord neurons
- Spinal nuclear calcium regulates a distinct genomic program in pain states
- C1q, a novel target of nuclear calcium signaling, induces synaptic spine remodeling
- Blockade of nuclear calcium signaling in spinal cord inhibits long-term inflammatory pain

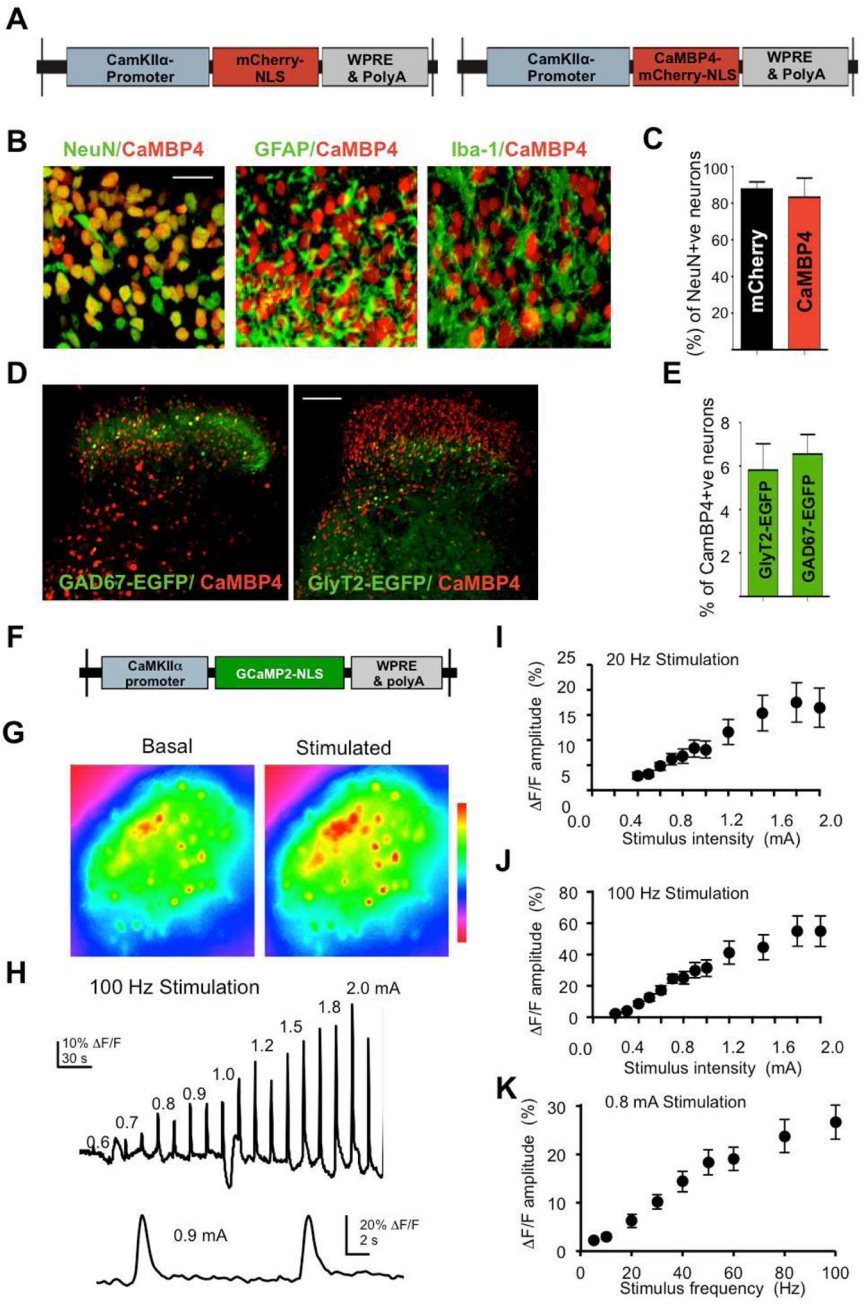

Fig. 1.

Viral vector mediated gene transfer to the lumbar spinal dorsal horn *in vivo*. (A) Schematic representation of two rAAVs: a nuclearly-targeted mCherry control (mCherry.NLS) and nuclear-localized, mCherry-tagged CaMBP4 (CaMBP4). (B) Co-expression of CaMBP4 with neuronal (NeuN), astrocytic (GFAP), and microglial (Iba-1) marker proteins in the spinal dorsal horn (scale bar = 50 μm). (C) Quantification of mCherry.NLS and CaMBP4 colocalization with NeuN in the spinal cord dorsal horn (L3–L5). (D, E) Typical expression patterns of CaMBP4 and EGFP in glycinergic (GlyT2-EGFP) or GABAergic (GAD67-EGFP) indicator mice (scale bar = 100 μm in D) and quantification of colocalization (E). (F, G) rAAV expressing genetically-encoded nuclear calcium indicator, GCaMP2.NLS and

nuclear calcium signals observed in dorsal horn neurons prior to (pre) and upon electrical stimulation of the ipsilateral dorsal root (post). (H) Typical ΔF/F trace of nuclear calcium transients evoked by 1 s, 100 Hz stimulation of the dorsal root. (I, J) Summary of data showing the relative amplitudes of nuclear calcium signals evoked by 1 s dorsal root stimulation of varying amplitudes at 20 Hz (n = up to 24 slices)(I) or 100 Hz (n = up to 18 slices)(J). (K) Summary data showing the relative amplitudes of nuclear calcium signals evoked by 1 s, 0.8 mA stimulus trains of varying frequency (n = up to 10 slices).

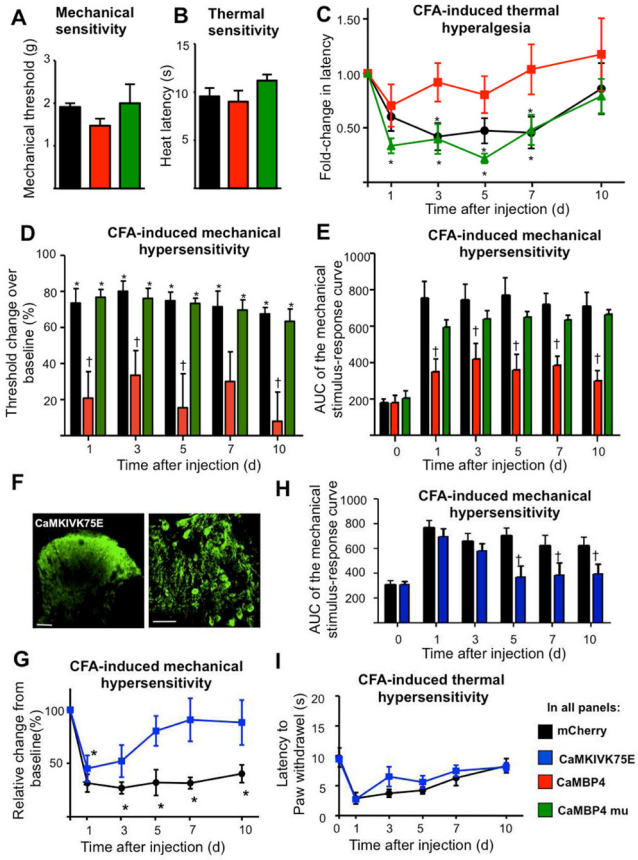

Fig. 2.

Inhibitors of nuclear calcium signaling in the spinal dorsal horn disrupt the development of inflammatory hyperalgesia, but have no influence on basal pain sensitivity. (A, B) Animals expressing mCherry (control, black symbols), functional CaMBP4 (red symbols), or an inactive mutant of CaMBP4 (CaMBP4mu, green symbols) were subjected to punctuate mechanical pressure stimuli (dynamic aesthesiometer in panel A) or radiant heat (plantar test with heat ramp in panel B). (C, D) Drop in paw withdrawal latency (C) or mechanical response thresholds (D) over time following CFA-induced unilateral hind paw inflammation on day 0. (* $P < 0.05$ relative to baseline; $^{\dagger}P < 0.05$ relative to mCherry; One-way ANOVA, post-hoc Dunnett's test). (E) Integrals of mechanical stimulus-response frequency curves for von Frey hair forces ranging from 0.07 to 2 g following unilateral hindpaw CFA injection († $P < 0.05$ relative to mCherry). (F) Anti-Flag immunohistochemistry showing localization of dominant-negative CaMKIV (CaMKIVK75E) in the spinal dorsal horn (scale = 100 μm, higher magnification in panel at the right, scale = 50 μm). (G, H) CFA-induced mechanical hypersensitivity in control mice and mice expressing CaMKIVK75E expressed as % change over baseline (G) or as integral of the entire von Frey stimulus intensity-response frequency curve (H) (* $P < 0.05$ relative to baseline; † $P < 0.05$ relative to mCherry; one-way ANOVA followed by Dunnett's test). (I) CFA-induced thermal hypersensitivity in control mice and mice expressing CaMKIVK75E (one-way ANOVA). In all panels, n = 8–10 mice/treatment group.

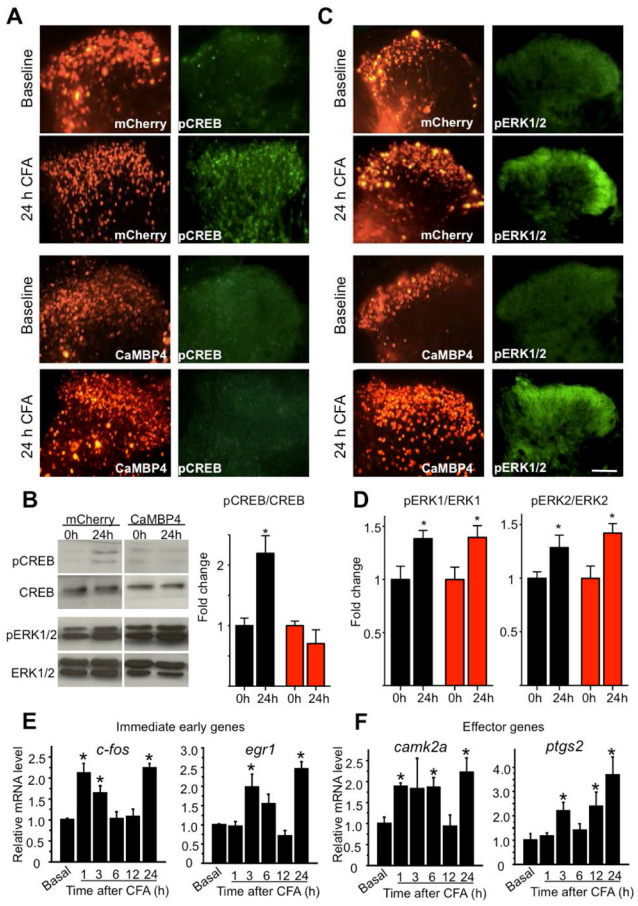

Fig. 3.

Contribution of nuclear calcium signaling in spinal dorsal horn neurons to phosphorylation of CREB (pCREB; panels A and B) and ERK1 as well as ERK2 (pERK1/2; panels C and D) in the spinal cord and temporal analysis of the course of gene following CFA-induced unilateral hindpaw inflammation. In panels A and C, identical sections are represented in both fluorescence channels per group. (A, B) Typical examples of immunoreactivity for pCREB (A) or Western blotting of pCREB and its densitometric quantification upon normalizing total CREB levels (B) in the spinal dorsal horn at 24 h after CFA injection as compared to basal state in mice spinally expressing mCherry or CaMBP4. (C, D) Typical examples of immunoreactivity for phosphorylated ERK1 and ERK2 (pERK1/2) in the spinal dorsal horn (C) or Western blotting of pERK1 and pERK2 and densitometric quantification upon normalizing total ERK1 or ERK2 levels (D) at 24 h after CFA injection over basal values in mice spinally expressing mCherry or CaMBP4 (* indicates $P < 0.05$ as compared to basal levels). Scale bars = 100 μm. In the above panels, n = 4–5 mice/treatment group. (E, F) Quantitative RT-PCR analysis of time course of upregulation of typical immediate-early genes (E) and gene encoding some typical effectors of nociceptive hypersensitivity (F) in spinal dorsal horn of wild-type mice following CFA-induced paw inflammation. n = at least 3 each. In all panels, ANOVA was performed followed by post-hoc Fisher's test. * represents $P < 0.05$ as compared to basal levels (0 h) and † indicates $P < 0.05$ as compared to the mCherry group

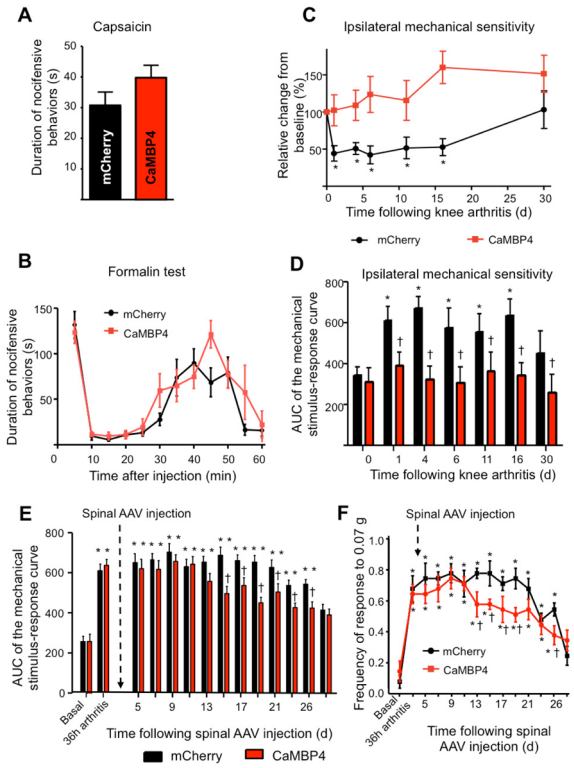

Fig. 4.

Effects of CaMBP4-induced disruption of spinal nuclear calcium signaling on behavioral manifestations of early nociceptive hypersensitivity (capsaicin test) and persistent inflammatory pain (knee arthritis model). Mice represented in panels A–D received AAV1/2-mediated spinal delivery of CaMBP4 (red symbols) or mCherry (black symbols) 4 weeks prior to being tested in the capsaicin or arthritis models. Mice represented in panels E and F received viral-mediated spinal delivery of CaMBP4 or mCherry at 36 h after induction of knee arthritis. (A, B) The cumulative durations of acute nocifensive behaviors evoked by intraplantar injection of capsaicin (A) or formalin (B) are shown ($P > 0.05$; Student's t-test). (C, D) Mechanical hypersensitivity following knee arthritis is represented as a change in mechanical threshold over baseline in % in panel C and as an integral of the entire von Frey stimulus intensity-response frequency curve over time after knee arthritis in panel D. In all of the above panels, n = 8–10 mice/treatment group. (E, F) Effects of spinal expression of mCherry (n= 8) or CaMBP4 (n= 8) using rAAVs injected two days after induction of knee arthritis. Mechanical hypersensitivity is represented as an integral of the entire von Frey stimulus intensity-response frequency curve over time after knee arthritis in panel E. Mechanical sensitivity of the same cohort of mice to a low-intensity von Frey stimulus of 0.07g is shown in panel F. In panels C–F, * indicates $P < 0.05$ as compared to baseline values and † indicates $P < 0.05$ as compared to the mCherry group; ANOVA was performed followed by post-hoc Dunnett's test.

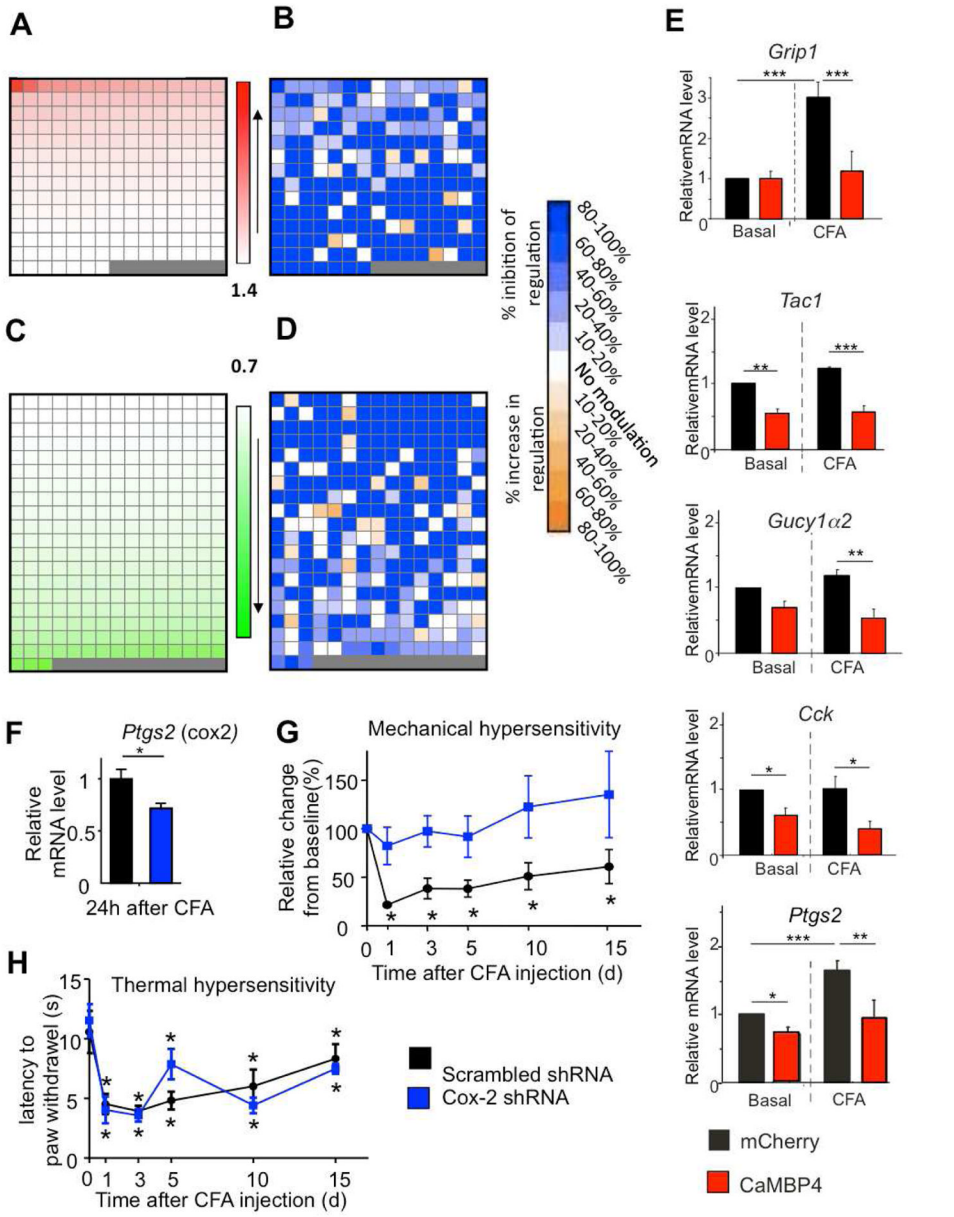

Fig. 5.

Representation of gene profiling data derived from spinal dorsal horns of CaMBP4-expressing mice and mCherry-expressing mice in the basal state or 24 h after CFA-mediated bilateral paw inflammation (n = 4 per group). (A–D) Representation of genes upregulated with a cut-off of 1.4 (A) or downregulated with a cut-off of 0.7 (C) in CFA-inflamed mice over basal state in mCherry mice. Changes in CFA-induced upregulation (B) or down-regulation (D) of individual genes by spinal expression of CaMBP4 are represented, segregated according to magnitude of modulation (color key on the extreme right; white fields represent CFA-regulated genes that are not affected by CaMBP4 expression). Each field in panels A & C represents 1 gene and the same gene is represented in corresponding fields in the panels B and D, respectively. See methods section for detailed description of the method of calculating % modulation of CFA-induced gene regulation by CaMBP4. (E) Validation of genes regulated in profiling experiments via quantitative reverse-transcriptase

PCR on cDNA derived from spinal dorsal horns of mice in the basal state and at 24 h after CFA-induced paw inflammation. (F) Attenuation of CFA-induced upregulation of *Ptgs2* gene encoding Cox-2 in the spinal dorsal horn of mice expressing an shRNA against *Ptgs2* in the spinal cord (Student's t-test). (G, H) Comparison of CFA-induced mechanical hypersensitivity (G) or thermal hyperalgesia (H) in mice spinally expressing shRNA against *Ptgs2* or control RNA (H); n = 8–10 mice/treatment group.* indicates $P < 0.05$ as compared to baseline values; ANOVA followed by post-hoc Dunnett's test.

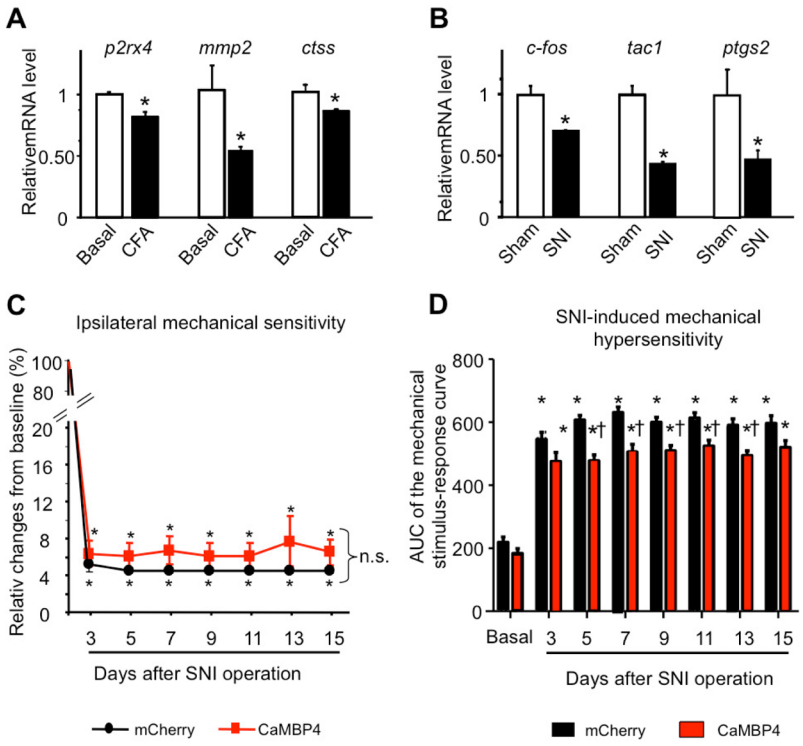

Fig. 6.

Analysis of the regulation of nuclear calcium-gene targets in models of peripheral inflammation (CFA) or neuropathy (spared nerve injury, SNI) and phenotypic characterisation of the influence of blockade of spinal nuclear calcium signaling on neuropathic pain. (A, B) Quantitative RT-PCR analysis of spinal expression of some neuropathic pain-associated genes at 24h post CFA and of some inflammatory pain-associated genes at 7 days after SNI (B)(n = 3 mice per condition in A & B). (C, D) Mechanical hypersensitivity following SNI is represented as a change in mechanical threshold over baseline in % in panel C and as an integral of the entire von Frey stimulus intensity-response frequency curve for von Frey hair forces ranging from 0.07 to 1 g over time after SNI in panel D; (n = 7–8) (* $P < 0.05$ relative to baseline, n.s.: non-significant, † $P < 0.05$ relative to mCherry).

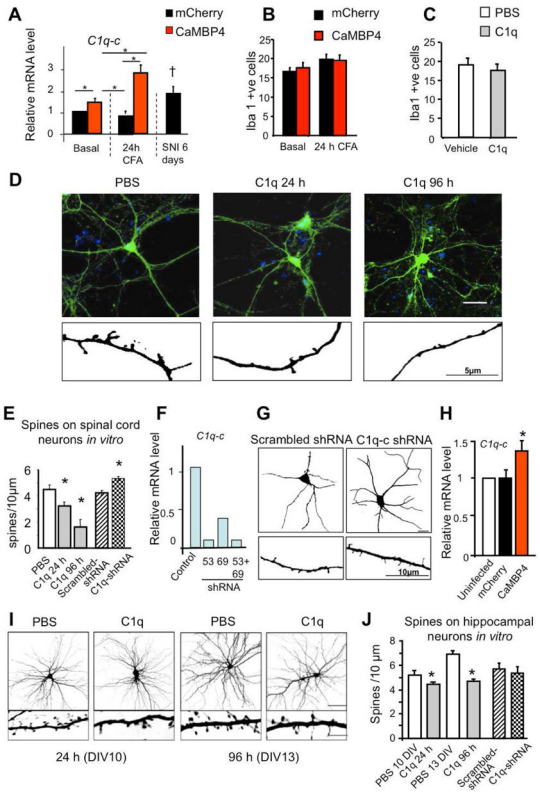

Fig. 7.

Analysis of C1q, a novel nuclear calcium target, its relation to spinal microglia and its role in dendritic spine remodelling in spinal and hippocampal neurons *in vitro*. (A) Quantitative RT-PCR analysis of spinal expression of C1q-c at 24 h after hindpaw injection of CFA and at 6 days after SNI over basal state in CaMBP4- or or mCherry-mice (n = 4 each). (B, C) Spinal microglia identified via Iba1-immunoreactivity in the spinal dorsal horns of control mice, inflamed mice and inflamed mice treated with intrathecal C1q (100 ng) for 48 h; n = 3 mice/group. (D, E) Typical examples (D) and quantitative summary (E) of morphometric analysis of EGFP-labeled synaptic spines on cultured, mature spinal cord neurons following treatment with C1q (100 ng) or vehicle over 24h–96h or following treatment with shRNA against C1q expression or control RNA (Scale bar = 50 μm in the upper panels, 5 μm in the lower panels; at least n = 3 different culture preparations). (F) QRT-PCR analysis of expression of the C1qc subunit of the trimeric C1q complex validating shRNA-mediated knockdown. (G) Typical examples of spinal neuronal morphology and spine density in spinal neurons with AAV-mediated downregulation of C1q expression as compared to controls. (H) QRT-PCR analysis of *C1q-c* expression in uninfected hippocampal neurons and in hippocampal neurons infected with rAAVs expressing the indicated proteins (n=4). * indicates $P < 0.05$ as compared to uninfected. (I, J) Typical examples (I) and quantitative summary (J) of morphometric analysis of EGFP-labeled synaptic spines on hippocampal neurons at 10 days or 16 days in vitro (DIV) (Scale bar = 20 μm in the upper panels and 5 μm in the lower ones) upon treatment with C1q (100 ng) or vehicle over 24h–96h or following viral expression of *C1q-c* shRNA or scrambled RNA. * $P < 0.05$ as compared to corresponding control. n= >600 spines counted, 12 neurons per condition, 3 independent culture preparations.

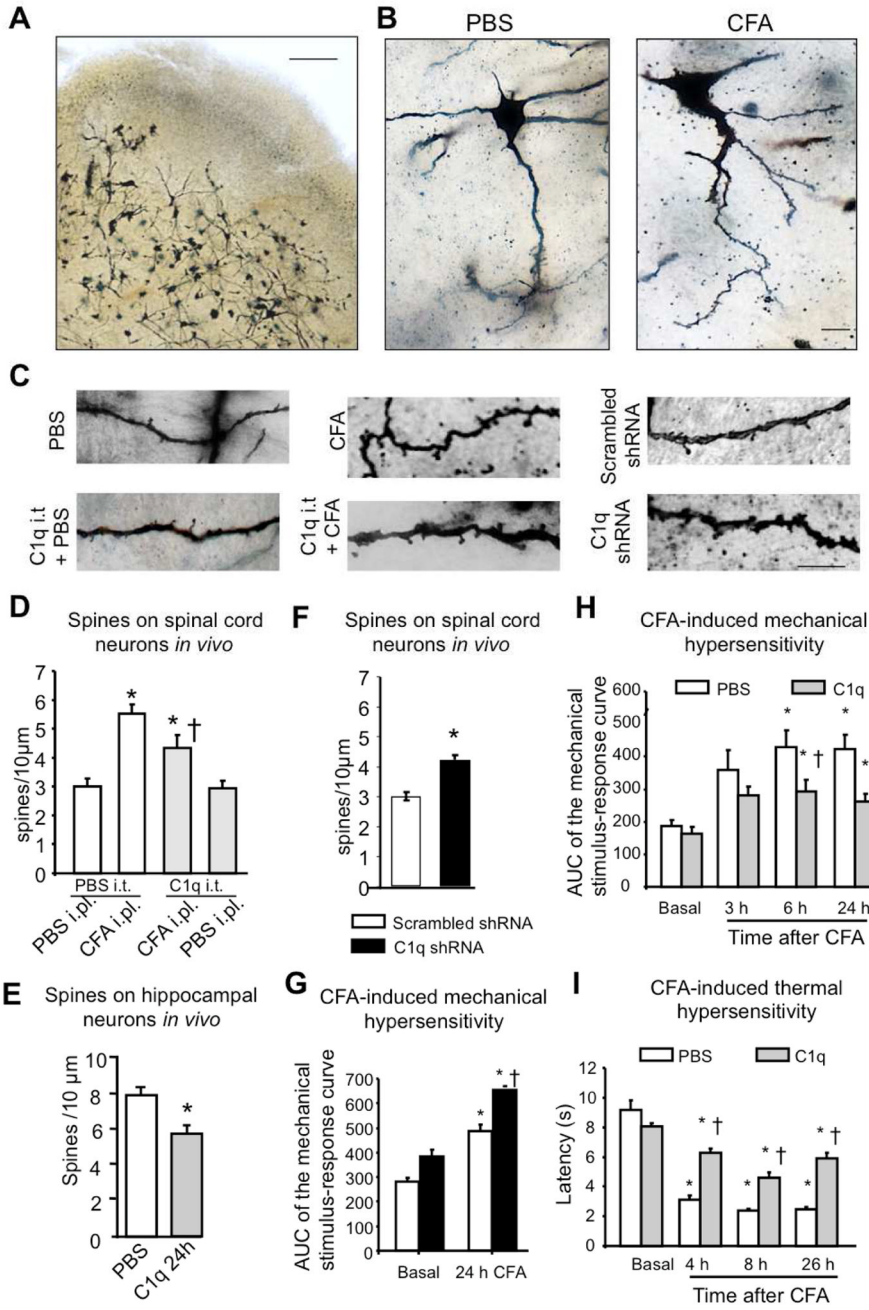

Fig. 8.

Spine remodelling in spine dorsal horn neurons following peripheral inflammation in vivo via the the novel nuclear calcium target, C1q, and its role in inflammatory pain hypersenstivity. (A) Typical example of Golgi staining on spinal dorsal horn slices with neurons labeled scross lamina II–V. Scale bar = 200 µm. (B) Typical examples of labelled neurons in mice injected intraplantar with PBS or CFA (24 h post-injection). Scale bar = 20 µm. (C) High magnification views of microscopic images of labelled dendrites with synaptic spines in mice with intraplantar injection of PBS or CFA (24 h) and treated intrathecally with vehicle or C1q (100 ng). Right hand panels represent images from mice with rAAV-mediated expression of C1q shRNA or scrambled RNA in spinal dorsal horn

neurons in vivo. Scale bar = 10 μm (D, E) Quantitative summary of synaptic spine density in spinal dorsal horn neurons (D) or in hippocampal neurons (E) *in vivo* following intrathecal injection (D) or direct intrahippocampal injection (E) of C1q (100 ng) (3–4 animals per condition, 20–30 neurons, 500–700 spines counted analysed spinal neurons; 2 animals per condition, 14 neurons, more than 600 spines analysed for hippocampal neurons). (F) Quantitative summary of synaptic spine density in spinal dorsal horn neurons in mice with rAAV-mediated expression of *C1q-c* shRNA or scrambled RNA (2 animals, 20 neurons per condition, 300–500 spines counted). (G, H) CFA-induced mechanical hypersensitivity in mice injected with rAAV-*C1qc-shRNA* or rAAV-*scrambled RNA* at 24 h (G) (n = 3–4/group) or in mice following intrathecal administration of recombinant C1q (100 ng) or vehicle 3-times over 24h period post-CFA (H) (n = 6 each group). In panels D, G, H & I, * indicates $P < 0.05$ as compared to baseline values within the same group and † indicates $P < 0.05$ as compared to the corresponding control group; in panels E & F, * $P < 0.05$ between the two groups ANOVA followed by post-hoc Dunnett's test.; In all panels, ANOVA followed by post-hoc Dunnett's test.